Journal of *Marine Science and Engineering*

MDPI

Article

Growth of the Mesopelagic Fish *Vinciguerria attenuata* (Cocco, 1838) in the Strait of Messina (Central Mediterranean Sea)

Francesco Longo [1,†], Danilo Malara [2,†], Emanuele Asciutto [1] and Pietro Battaglia [1,*]

[1] Department of Integrative Marine Ecology (EMI), Stazione Zoologica Anton Dohrn, National Institute of Biology, Ecology and Marine Biotechnology, Sicily Marine Centre, c/o Villa Pace, Contrada Porticatello 29, 98167 Messina, ME, Italy; francesco.longo@szn.it (F.L.); emanuele.asciutto@szn.it (E.A.)

[2] Department of Integrative Marine Ecology (EMI), Stazione Zoologica Anton Dohrn, National Institute of Biology, Ecology and Marine Biotechnology, Calabria Marine Centre, C.da Torre Spaccata, 87071 Amendolara, CS, Italy; danilo.malara@szn.it

* Correspondence: pietro.battaglia@szn.it

† These authors equally contributed to the manuscript.

Abstract: The age and growth of the slender lightfish *Vinciguerria attenuata* are investigated for the first time by the analysis of otolith microstructure. A total of 242 individuals (standard length range = 15.3–39.0 mm) are collected from the Strait of Messina (central Mediterranean Sea). The analysis of the length–weight relationship highlights a hyper-allometric growth for all specimens, while when males and females are analyzed separately, the results point out an isometric growth for males and hyper-allometric growth for females, although no statistical differences emerge comparing sex curves (p-value = 0.06). Microincrement readings are considered valid only for 214 sagittal otoliths. Microincrement counts range from 31 to 49 (average = 39.9) in the otolith central zone, 28 to 53 (average = 43.2) in the middle zone, and 15 to 332 (average = 136.1) in the external zone. Overall, total microincrements range between 75 and 418. Different growth models (von Bertalanffy, Gompertz and logistic models) are taken into account to select the best-fitting model in describing the growth patterns in *V. attenuata*. The logistic growth model is selected as the best-fitting model, and its parameters for all individuals are L_∞ = 38.597, k = 0.0104 and I = 122.4.

Keywords: otolith; microincrements; length–weight relationship; growth model; Phosichthyidae; Mediterranean

Citation: Longo, F.; Malara, D.; Asciutto, E.; Battaglia, P. Growth of the Mesopelagic Fish *Vinciguerria attenuata* (Cocco, 1838) in the Strait of Messina (Central Mediterranean Sea). *J. Mar. Sci. Eng.* **2023**, *11*, 1055. https://doi.org/10.3390/jmse11051055

Academic Editor: Dariusz Kucharczyk

Received: 21 April 2023
Revised: 10 May 2023
Accepted: 11 May 2023
Published: 15 May 2023

1. Introduction

Phosichthyidae is a fish family that mainly includes mesopelagic and bathypelagic species, also known as "lightfishes". These species possess luminous organs (photophores) located in the ventral part of the body and are characterized by a very small size. For this reason, they generally lack any commercial value, and their stocks have not yet been exploited by fisheries. Overall, 24 species belonging to the genera *Ichthyococcus*, *Phosichthys*, *Pollichthys*, *Polymetme*, *Vinciguerria*, *Woodsia*, and *Yarrella* are attributed to the Phosichthyidae, but only *Ichthyococcus ovatus*, *Vinciguerria attenuata*, and *Vinciguerria poweriae* are found in the Mediterranean Sea. The biology and ecology of lightfishes, as well as their life history traits, are poorly known, and scientific knowledge is often limited to few areas/species. Most of the available information on lightfishes relates to their distribution and diversity and comes from research cruises in open waters (e.g., [1–6]). Lightfishes are important components of the deep scattering layer (DSL), although each species displays a different behavior. The not-migrant or weakly migrant *I. ovatus*, *V. attenuata*, and *V. poweriae* usually make very short vertical movements, preferring 400 m DSL regardless the photoperiod, as observed in Mediterranean and Atlantic waters [6–9]. In contrast, *Vinciguerria lucetia* and *Vinciguerria nimbaria* [3,4,10–13] can perform wider diel

vertical migrations in oceanic waters, although in some areas also display an unusual behavior, consisting in the permanence of some schools at upper layers during daylight. Several studies provided evidence that in certain areas some lightfishes are among the dominant component of micronekton communities. For instance, the acoustically estimated biomass of *V. lucetia* varies between 2 and 11 million tons off the coasts of Peru, within the Humboldt Current (Pacific Ocean) [3], while Menon et al. [14] observed a high abundance of *V. nimbaria* in the mesopelagic community of the Indian Ocean. In Mediterranean waters, Battaglia et al. [15] found that *V. attenuata* is one of the most abundant mesopelagic fish in the upwelling area of the Strait of Messina by analyzing the species composition and abundance of stranded deep fauna.

The abundance of lightfishes in mesopelagic waters represents an important available food resource for various marine predators. According to some studies [11,12,16], the unusual high concentration of *V. nimbaria* at upper layers during daylight attracts tunas (*Katsuwonus pelamis* and juveniles of *Thunnus albacares* and *Thunnus obesus*) off African coasts (equatorial Atlantic Ocean), also supporting a seasonal tuna fishery. A strict trophic relationship between *V. lucetia* and the jumbo squid *Dosidicus gigas* has also been observed; indeed, some scientists demonstrated that the migratory movements of this cephalopod predator are closely related to the distribution of lightfish prey (*V. lucetia*) in the Humboldt Current system of Peru [17]. Moreover, in the central Mediterranean Sea, the lightfish *V. attenuata* is an important prey item in the pelagic food web of the Strait of Messina for predators of different trophic levels, such as the mesopelagic fish *Chauliodus sloani* [18], the carangid *Trachurus picturatus* [8], and to a lesser extent, the bluefin tuna *Thunnus thynnus* [19,20].

Lightfishes likely have a short life cycle, as highlighted by Tomás and Panfili [21] who observed a lifespan of less than one year in *V. nimbaria*. However, *V. nimbaria* can attain shorter sizes (about 5 cm SL) than other members of Phosichtyidae, which can reach 20–30 cm of total length [22], so larger species could live longer. The short life cycle of lightfishes may explain the extended duration of their spawning period, which lasts several months [2,13,23,24] to ensure the population regeneration. Age and growth data on lightfishes are very limited, and if we exclude the above cited study [21], there is little available information regarding length–weight relationships [14,25–27] and ontogenetic changes in otolith growth [28]. These data are important to describe essential life history traits of these species.

For this reason, the aim of this paper is to examine the growth of the slender lightfish *V. attenuata* through the analysis of microincrements in the otolith microstructure. We here describe the growth patterns by the estimation of the best-fitting growth curve among the most common growth models (Gompertz, von Bertalanffy, and logistic) and the analysis of the length–weight relationship.

2. Materials and Methods

2.1. Sample Collection and Measurements

The sample collection was carried out along the coast of the Strait of Messina (central Mediterranean Sea; Figure 1), where complex hydrodynamic phenomena periodically cause the stranding of mesopelagic fish fauna [15]. Out of a total of 242 individuals, we excluded 28 specimens since the otoliths were unreadable or the standard error in readings exceeded the threshold limit (see Section 2.4); therefore, the study was performed on 214 individuals. According to Longo et al. [29], only fresh and undamaged animals were taken into consideration, avoiding errors deriving from accidental weight loss caused by dehydration.

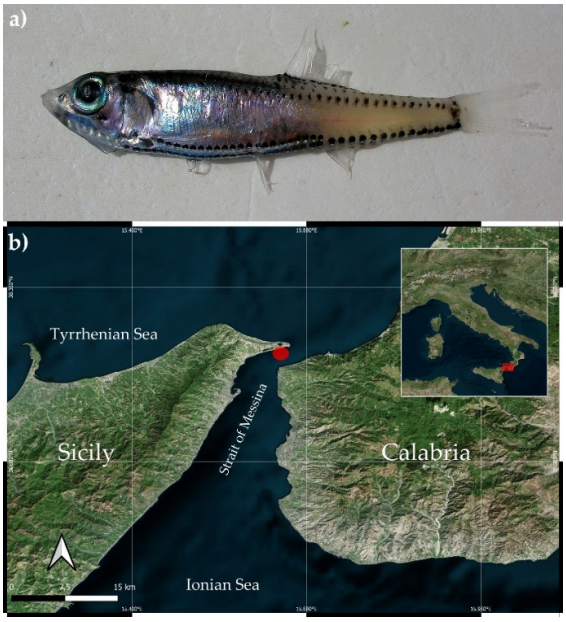

Figure 1. Specimen of *Vinciguerria attenuata* (**a**) and study area located in the Strait of Messina (**b**).

In the laboratory, morphometric (standard length, SL) and ponderal (body mass, W) measurements were recorded to the nearest 0.1 mm and 0.01 g, respectively. Animals were sexed by observing the gonads with a light microscope, after positioning gonadal tissues on a glass slide and using a coverslip to obtain clear images.

2.2. Length–Weight Relationship

The *W-SL* relationship was calculated for all individuals and for each sex (female and male) separately. The *a* and *b* parameters were obtained by log-transforming the equation $W = a\,(SL^b)$, where *W* is the body mass (g), *SL* is the standard length (mm), *a* is the intercept, and *b* is the slope [30–32]. The model homoscedasticity and normality assumption were visually checked using the R package olsrr (v. 0.5.3; [33]. The fish allometric or isometric growth [34] was assessed by comparing the slope *b* to the isometric value of 3 by Student's *t*-test (one-sample *t*-test) and checking the presence of significant differences ($\alpha = 0.05$), while the differences between gender were performed by a Welch two-sample *t*-test comparing the female and male *b* values (b_F and b_M) from the respective *W-SL* equations. Statistical analyses were conducted using R software (v. 4.1.1) and R-studio environment (v. 2023.03.0) [35,36].

2.3. Otolith Extraction and Preparation

Sagittal otoliths were removed, cleaned, coded, and stored dry. The otolith size was recorded by [25,26]: (i) the maximum distance between the anterior otolith tip to the posterior edge (maximum length, OL); (ii) the maximum distance between the dorsal and ventral margin (maximum height, OH). These measures were taken with an accuracy of 0.01 mm, using a stereomicroscope (Carl Zeiss, model Stemi 508, Germany) equipped with a camera (Axiocam 305 color, ZEISS, Germany). Post-processing images were analyzed by ZEN blue edition (v. 3.1.0, ZEISS, Germany) digital image software.

The relationship between OH/OL and fish SL was assessed using the linear regression model. The linear model assumptions of normality and homogeneity were checked based on visual observation of the graphical plot of standardized residuals vs. theoretical quantiles and residuals vs. fitted values, respectively [37].

Thin sagittal sections were obtained, mounting the otoliths on slides with Eukitt® mounting medium and using a grinding/polishing machine (Remet LS2), according to Longo et al. [29].

2.4. Otolith Readings, Increments' Interpretation and Analysis

Otolith sections were observed by a light microscope (ZEISS Axioscop2, Germany), and their images were acquired and analyzed using the Axiocam 208 color camera (ZEISS, Germany) and ZEN blue edition (v. 3.1.0, ZEISS, Germany) digital image processing software. The growth pattern was observed to distinguish zones of similar structure in the otolith sagittal section, and the presence of different distinctive incremental zones was assessed, also comparing our observations with otolith images reported in other studies (e.g., Tomás and Panfili [21] for Phosichthyidae; Longo, et al. [29] and references herein cited for other mesopelagic fishes). On the basis of the different growth patterns found in the sagittal section, we distinguished three growth zones: central (CZ), middle (MZ), and external (EZ) zones (the description of the otolith zones is reported in the results section). Microincrements count for each otolith zone started from the first noticeable increment after the central primordium to the otolith edge [29,38,39]. For lanternfishes, these otolith regions usually correspond to the larval zone (LZ), post-larval zone (PLZ), and post-metamorphic zone (PMZ), respectively [40–42], but in the present paper we prefer to avoid referring to otolith growth zones using terms related to the life history because there are very few studies on Phosichthyidae and an accurate validation of daily growth increments has not been done yet. On the other side, although Tomás and Panfili [21] used the same precautionary approach, they refer to microincrements in the otolith structure of the congeneric species *Vinciguerria nimbaria* maybe having a daily-like formation. Furthermore, Sassa and Takahashi [43] postulated that the increments observed in the larval otoliths of *V. nimbaria* were deposited daily, although further validation of this relationship is needed in the future. For these reasons, in the present paper, the results of the readings are reported in terms of the number of observed microincrements and not daily rings.

Readings in each otolith zone were performed counting the microincrements three times, and the average value was considered for analysis; however, the otoliths were discarded if the standard error for the three readings was higher than 5 [29,39].

2.5. Growth Models

Growth of *V. attenuata* was evaluated by a multi-model inference (MMI) approach [44,45]. Thus, data were fitted into von Bertalanffy, Gompertz, and logistic models to obtain growth assessments for all individuals (general model), as well as for sexes (female and male models) separately:

Gompertz growth model [46]:

$$SL = L_{\infty} e^{\left(-e^{(-k(x-I))}\right)} \quad (1)$$

von Bertalanffy growth model [47]:

$$SL = L_{\infty}\ (1 - \ e^{(-k\ (x-t_0))}) \quad (2)$$

Logistic growth model [34,48]:

$$SL = \ L_{\infty}\left(1 + e^{(-k(x-I))}\right)^{-1} \quad (3)$$

where SL = standard length at age t, L_{∞} = theoretical asymptotic length, t_0 = theoretical age when the body length is equal to 0, k = growth rate at which SL approaches L_{∞}, and I = age at inflection point. For each model, the FSA package (v. 0.9.4; [49]) and "nlstools" package (v. 2.0.0; [50]) were used to determine the coefficients' starting values (L_{∞}, K, t_0 or I) and the bootstrapping confidence intervals (999 iterations), respectively. Furthermore, the selection of the best-performing model was based on the Akaike's information criterion

in its small-sample bias-corrected form (AICc; [51,52]) by using an AICcmodavg package (v. 2.3-2; [53]). Our approach was to consider the model with the lowest AICc value as the best-performing one. However, when the Delta AICc (difference between AICc of two models) resulted <2, the model with the highest AICc weight value was selected. Differences between growth curves were investigated using the Welch two-sample *t*-test (α = 0.05) amongst the female and male growth parameters (L_∞, K, t_0 or I). Statistical analyses and graphs were produced using R software (v. 4.2.2) and R-studio environment (v. 2023.03.0) [35,36].

3. Results

Overall, the size (SL) of individuals ranged from 15.3 to 39.0 mm (mean ± standard deviation = 27.27 ± 5.64 mm), while the body mass (W) varied between 0.02 and 0.86 g (mean ± standard deviation = 0.24 ± 0.16 g). Out of a total of 214 *V. attenuata*, 103 were females with a size range of 19.8–39.0 mm (mean ± standard deviation = 28.66 ± 4.92 mm) and a body mass between 0.04 and 0.86 g (mean ± standard deviation = 0.27 ± 0.16 g). Males (n = 87) were less abundant than females, and their size varied from 19.8 to 37.1 mm (mean ± standard deviation = 28.22 ± 4.67 mm), with a body mass ranging from 0.08 to 0.59 g (mean ± standard deviation = 0.25 ± 0.14 g) (Table 1). Finally, the sex was not determined in 24 small individuals. Figure 2 shows the length frequency distribution of *V. attenuata* by sex; in this graph, it is possible to observe that most samples are distributed within 20–35 size classes.

Table 1. Summary of size and weight ranges, mean, standard deviation (SD), and confidence interval (CI) values for all individuals, females, and males.

	All Individuals		Females		Males	
	Standard Length (mm)	Weight (g)	Standard Length (mm)	Weight (g)	Standard Length (mm)	Weight (g)
Min	15.30	0.02	19.80	0.04	19.80	0.080
Max	39.00	0.86	39.00	0.86	37.10	0.590
Mean	27.27	0.240	28.66	0.274	28.22	0.251
SD	5.642	0.157	4.917	0.162	4.669	0.135
Lower CI	26.517	0.219	27.711	0.243	27.241	0.223
Upper CI	28.029	0.261	29.61	0.305	29.203	0.280

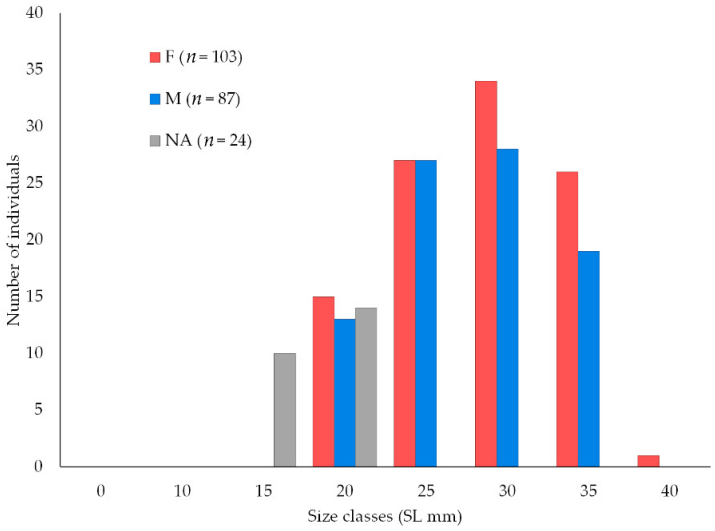

Figure 2. Length frequency distribution by sex of the studied sample of *Vinciguerria attenuata*.

The length–weight relationship analysis of *V. attenuata* (Figure 3) pointed out an allometric growth in the general model (t_{all} = 4.957, df = 2, *p*-value = 0.038). A similar result was observed for females (t_F = 4.563, df = 2, *p*-value = 0.045), while the male W-SL relationship was isometric (t_M= 0.722, df = 2, *p*-value = 0.546). However, the Welch two-sample *t*-test did not show statistically significant differences between female and male slopes (b_F = 3.599 and b_M = 3.098, respectively), accepting the hypothesis that $b_F = b_M$ (t = 2.607, df = 3.983, *p*-value = 0.06) and underlining that there was not a body shape dissimilarity between sexes.

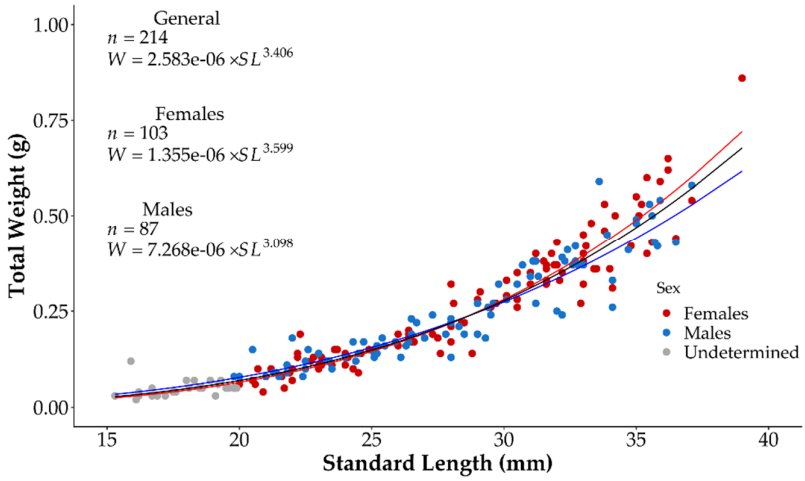

Figure 3. Length–weight relationship for total individuals (3a), males and females (3b) of *Vinciguerria attenuata.*

The relationship between otolith size and standard body length for *V. attenuata* was linear (Figure 4). Both OL-SL and OH-SL relationships provided a value higher than 0.9 for the coefficient of determination.

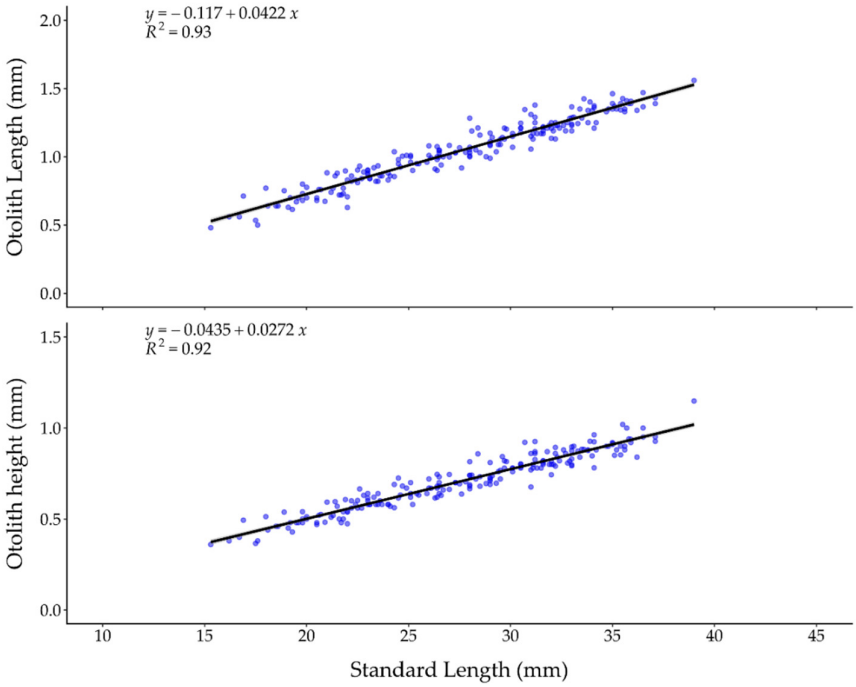

Figure 4. Fish length (SL mm) vs. otolith size (OL and OH) relationships in *Vinciguerria attenuata.*

The analysis of the growth patterns indicated the presence of three main growth regions comparable with the central (CZ), middle (MZ), and external (EZ) zones (Figure 5). Growth increments around the central primordium (Figure 5A) gradually increase in width (Figure 5C) toward the CZ margin, delimitated by a dark mark (Figure 5B), probably a metamorphic check. The MZ was darker than the other otolith regions, with larger "double" growth increments (Figure 5B). The EZ was characterized by a regular growth pattern, with microincrements becoming thinner moving toward the otolith margin (Figure 5D). In this otolith region, the growth increments were more easily readable.

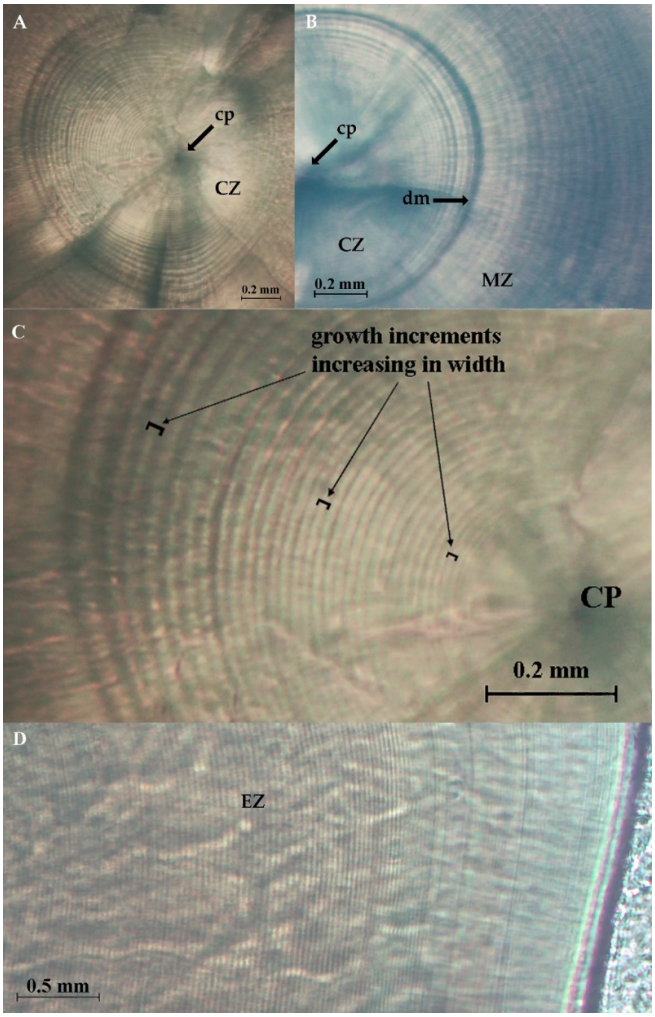

Figure 5. Microincrements in the sagittal section of the otolith of *Vinciguerria attenuata*: (**A**) particular of the central zone (CZ), with microincrements laid down a central primordium (cp); (**B**) dark mark (dm) between central (CZ) and middle (MZ) zones—larger microincrements characterize the MZ; (**C**) particular of the growth increments pattern, showing the increase in width from the central primordium to the marginal part of the nucleus; (**D**) regular growth microincrements observed in the external zone (EZ).

The microincrement counts ranged from 31 to 49 (average = 39.9) in the otolith central zone (CZ), 28 to 53 (average = 43.2) in the middle zone (MZ), and 15 to 332 (average = 136.1) in the external zone (EZ). Overall, total microincrements ranged between 75 and 418.

The MMI approach suggested that the best-fitting growth curve (starting values in Table 2) was the logistic growth model [34,48], which had the lowest AICc and delta values (Table 3).

Table 2. Starting values of the growth models for all datasets and for each gender. L_∞ = the theoretical asymptotic length, t_0 = theoretical age when the body length is equal to 0, and k = the growth rate at which SL approaches L_∞, whereas I = the age at inflection point.

	Starting Values		
	L_∞	k	t_0/I
All	33	0.02	58.596
Females	33	0.02	105
Males	33	0.04	150

Table 3. Model selection based on AICc, delta AICc, and AICc weight (AICcWt) results for the general (all data) and gender data relative to the Gompertz, von Bertalanffy (VBGM), and logistic models.

	Model Selection Based on AICc							
		K	AICc	Delta_AICc	AICcWt	Cum.Wt	LL	
All data	Logistic	4	706.61	0.00	0.58	0.58	−349.21	Support data and best model
	Gompertz	4	707.40	0.79	0.39	0.97	−349.60	Support data
	VBGM	4	712.72	6.11	0.03	1.00	−352.26	Less support data
Females	Logistic	4	350.33	0.00	0.54	0.54	−170.96	Support data and best model
	Gompertz	4	351.37	1.05	0.32	0.86	−171.48	Support data
	VBGM	4	353.09	2.76	0.14	1.00	−172.34	Less support data
Males	Logistic	4	273.41	0.00	0.44	0.44	−132.46	Support data and best model
	Gompertz	4	273.85	0.44	0.35	0.79	−132.68	Support data
	VBGM	4	274.90	1.49	0.21	1.00	−133.20	Less support data

Growth curves and model parameters are shown in Figure 6 and Table 4, respectively. The parameters for the general curve were L_∞ = 38.597, k = 0.0104, and I = 122.4, whereas the gender parameters estimated were: L_∞ = 39.45, k = 0.0095, and I = 121.4 for females and L_∞ = 39.34, k = 0.0094, and I = 120.7 for males. The growth was similar in females and males without any sex growth dissimilarity (Welch two-sample t-test p-value for all parameters >0.05; Table 5).

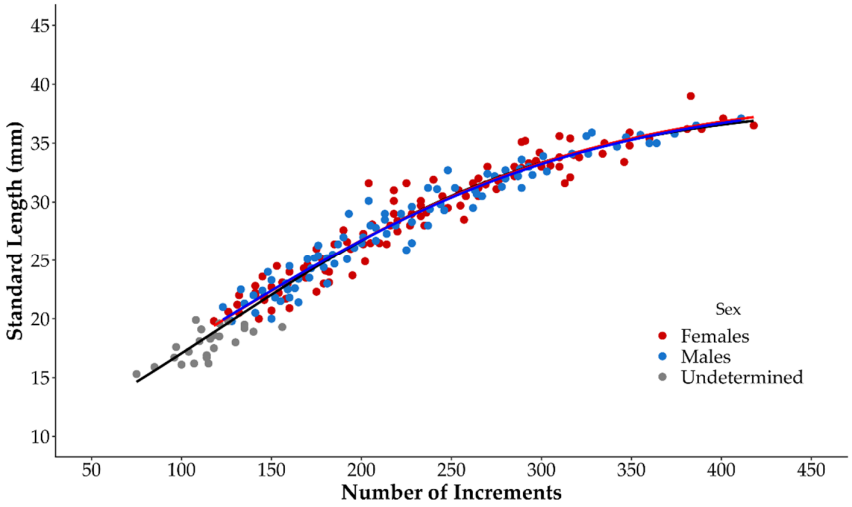

Figure 6. Relationship between the standard length and the number of increments observed in the otoliths of *Vinciguerria attenuata*. Data were fitted to a logistic growth model.

Table 4. Best-fitting model's parameters of all individual, female, and male growth curves. Information includes L_∞, k, and I estimate, lower and upper 95% confidential interval (C. I.), and standard errors.

Best Model Parameters All Data							
Growth Data	**Parameters**	**Estimate**	**Lower 95% C.I.**	**Upper 95% C.I.**	**Std. Error**	***t* value**	**Pr(>|t|)**
All data	L_∞	38.597	37.58	39.94	0.59	65.28	$<2 \times 10^{-16}$
	k	0.0104	0.0095	0.011	0.00048	21.61	$<2 \times 10^{-16}$
	I	122.4	117.39	128.58	2.782	43.99	$<2 \times 10^{-16}$
	Residual standard error	1.246 on 211 degrees of freedom					
Females	L_∞	39.45	37.66	42.190	1.115	35.38	$<2 \times 10^{-16}$
	k	0.0095	0.0078	0.011	0.00085	11.13	3.23×10^{-7}
	I	121.4	113.6	133.61	4.84	25.11	$<2 \times 10^{-16}$
	Residual standard error	1.291 on 100 degrees of freedom					
Males	L_∞	39.34	37.64	42.12	1.15	34.15	$<2 \times 10^{-16}$
	k	0.0094	0.0077	0.011	0.00088	10.76	5.42×10^{-8}
	I	120.7	112.6	132.85	4.810	25.00	$<2 \times 10^{-16}$
	Residual standard error	1.129 on 84 degrees of freedom					

Table 5. Welch two-sample *t*-test to compare male and female age at length curves parameters.

	T	**df**	***p*-Value**
L_∞	−0.041	3.000	0.969
t_0	−0.058	3.998	0.957
I	−0.118	3.999	0.912

4. Discussion

This paper examined for the first time the growth of *V. attenuata* through the analysis of the otolith microstructure and estimation of growth models.

Our findings revealed that the length–weight relationship for all individuals was hyper-allometric ($b > 3$). However, when sexes were considered separately, the LW

relationship resulted in being isometric in male and hyper-allometric ($b > 3$) in females, though no statistical differences were found during the comparison between sex curves. Although differences in b values between sexes could be explained by a different sample size, we believe that the presence of heavier gonads in larger mature females may have resulted in an allometric growth estimate. In fact, the female and male curves (Figure 3) diverged in their final portion when length and weight were above 30 mm and 0.25 g, respectively. Such results are supported by the findings of López-Pérez et al. [27], who analyzed the SL-W relationship in *V. nimbaria*. In this study, the b value was higher (>3) when the curve was constructed using the wet total weight but became isometric when the authors used the eviscerated weight, demonstrating that gonads and/or gut content might influence this estimate [27]. Furthermore, in the congeneric species *V. nimbaria*, female gonads can reach up 0.45 g of weight in larger individuals [13]; therefore, it is very likely that the gonad mass influenced the weight in larger females.

Observation on the otolith microstructure highlighted the presence of different growth patterns that can be distinguished in three main otolith regions analogous to the central (CZ), middle (MZ), and external (EZ) zones found in lanternfish [1,10,29,39,54–57]. On the other hand, the analysis of otolith growth patterns showed some differences between our results and the findings of Tomás and Panfili [21], i.e., the only other study that investigates the growth in a species of the genus *Vinciguerria*. These authors observed five distinct zones (named I, II, III, IV, and V) in the transverse section of the otolith of *V. nimbaria* from the tropical Atlantic Ocean. Zone I contained 4–12 narrow microincrements, followed by zone II with similar microincrements but larger than the first ones. The boundary between zones I and II was a darker D-zone followed by a thin microincrement. Double microincrements characterized zone III, whereas zone IV was described as an area of intense growth (6–8 increments). Zone V had microincrements with variable width but with a quite regular pattern of deposition [21]. In our samples, the nucleus did not show differentiated zones, but microincrements laid down around the central primordium gradually increased in width up to a dark mark (dm), i.e., the boundary between nucleus (CZ) and the following growth zone with "double microincrements" (MZ). Therefore, zones I and II observed by Tomás and Panfili [21] in *V. nimbaria* probably correspond to the entire CZ in otoliths of *V. attenuata*. The presence of "double microincrements", as well as a deposition pattern characterized by an intense growth, suggests that the MZ in otolith of *V. attenuata* could correspond to zones III and IV described by Tomás and Panfili [21] in *V. nimbaria*. The EZ, on the other hand, is comparable with zone V, both characterized by a regular growth pattern and more readable increments.

Differences in growth increment deposition in congeneric species such as *V. attenuata* and *V. nimbaria* may be due to different causes related, for example, to environmental conditions or migrating behavior. As observed in the western Mediterranean basin [6], *V. attenuata* does not perform extensive diel migrations to the upper layers and can be usually found at the 400 m deep scattering layer (DSL), where the water temperature is essentially homogeneous (about 13 °C). In contrast, *V. nimbaria* usually makes diel vertical migrations between the sea surface (at night) and oceanic mesopelagic waters (around 400 m at day) [10,58], although the anomalous occurrence of *V. nimbaria* at 70–110 m during the day was also observed in the eastern tropical Atlantic Ocean [11,21].

Interpretation of growth marks in otoliths is not straightforward, especially in species where a validation of microincrement deposition has not yet been performed. They may be due to special events in the life history of the species (such as metamorphosis), changes in habitat, metabolism rate, fish behavior, or environmental conditions (e.g., lunar marks) [40,55,59]. Presumably, the dark mark observed between CZ and MZ is a metamorphic check (passage from larval stage to post-larval stage) usually associated to a habitat shift, as often found in other mesopelagic fish [40,55,60,61].

Furthermore, the deposition of "double microincrements" found in the MZ of mesopelagic fish was attributed by Gartner [42] to the period in which post-larvae migrate from upper waters to deep-sea habitat, just before metamorphosis. The most common

interpretation of these double increments is that they should be considered as a single primary microincrement [21].

The observation of otoliths with the light microscope allowed us to record a maximum number of 418 microincrements. Studies on the microstructure of the otoliths in Phosichthyidae are basically lacking, and age estimation for these species is quite difficult because the daily deposition of microincrements has not yet been validated [21]. However, if we assume that the microincrements observed in *V. attenuata* otoliths are formed daily, it could be hypothesized that the species has a lifespan of a little more than one year.

The application of the MMI approach [29,44,45] to our data showed that the logistic curve was the best-performing model to describe the growth of *V. attenuata*, although the Gompertz model also well-supported these data. The two types of growth are very similar; however, the Gompertz growth is generally faster in the early stages, while the logistic model shows a faster growth in older individuals [34,62]. In addition, as observed for other species [63], the logistic model describes better the growth in small-size and fast-growing species, while the Gompertz model fits better species of different size with moderate growth. This information is in line with our findings showing a rapid growth and small sizes in *V. attenuata*, but we also believe that the growth in this species is influenced by the body shape. In fact, *V. attenuata* tends to grow more in length and less in width (slim shape). Finally, it must be noted that our results are based on the available information collected and the growth models utilized in the MMI approach. In our samples, we collected both very young and older individuals; the possibility to examine all life stages has an important impact on the growth parameter estimates and, therefore, influence the choice of the best-fitting growth model [64].

Finally, the estimation of the length–weight relationship, the analysis of growth patterns, and the assessment of the best-fitting growth model for *V. attenuata* are useful to characterize different aspects of the life history traits of this species. Although a validation of microincrement deposition has not yet been performed in lightfishes, these data represent the first baseline for the future estimation of age and mortality rate in a Mediterranean population of *V. attenuata*. The description of life history traits has a key role in understanding the productivity and dynamics of fish populations [65] and in generating information useful to lay the basis of sustainable use of fish resources [66]. Thus, this study contributes to filling the information gap on some aspects of the biology of *V. attenuata*, producing data useful to assess the status of this fish resource. Given the importance of lightfishes in the marine trophic web, as well as the recent attempts of fishery exploitation of mesopelagic fish resources, it is advisable to collect biological and ecological data on the stocks of these species to allow a proper management of these important key-role prey.

Author Contributions: Conceptualization, P.B.; methodology, F.L., D.M., P.B.; software, D.M.; formal analysis, F.L., D.M., E.A., P.B.; investigation, F.L., D.M., E.A., P.B.; resources, P.B.; data curation, F.L., D.M., P.B.; writing—original draft preparation, P.B., F.L., D.M.; writing—review and editing, F.L., D.M., E.A., P.B.; supervision, P.B. All authors have read and agreed to the published version of the manuscript.

Funding: This research received no external funding.

Institutional Review Board Statement: Ethical review and approval were waived for this study because of the samples being already dead at the time of collection. *V. attenuata* specimens were collected stranded on the Sicilian coast of the Strait of Messina.

Informed Consent Statement: Not applicable.

Data Availability Statement: The data presented in this study are available on request from the corresponding author.

Conflicts of Interest: The authors declare no conflicts of interest.

References

1. Gjøsæter, J.; Kawaguchi, K. A Review of the World Resources of Mesopelagic Fish. FAO Fish. Tech. Pap. **1980**, 193, p. 157, ISBN 9251009244.
2. Krefft, G. Taxonomy and distribution of the fish-genus *Ichthyococcus* (Bonaparte, 1841) (Photichthyidae Weitzman, 1974) in the Atlantic Ocean. *Investig. Pesq.* **1983**, *47*, 295–309.
3. Cornejo, R.; Koppelmann, R. Distribution patterns of mesopelagic fishes with special reference to *Vinciguerria lucetia* Garman 1899 (Phosichthyidae: Pisces) in the Humboldt Current Region off Peru. *Mar. Biol.* **2006**, *149*, 1519–1537. https://doi.org/10.1007/s00227-006-0319-z.
4. Goçalo, C.G.; Katsuragawa, M.; Silveira, I.C.A.d. Patterns of distribution and abundance of larval phosichthyidae (actinopterygii, stomiiformes) in southeastern Brazilian waters. *Braz. J. Oceanogr.* **2011**, *59*, 213–229.
5. Olivar, M.P.; Hulley, P.A.; Castellón, A.; Emelianov, M.; López, C.; Tuset, V.M.; Contreras, T.; Molí, B. Mesopelagic fishes across the tropical and equatorial Atlantic: Biogeographical and vertical patterns. *Prog. Oceanogr.* **2017**, *151*, 116–137. https://doi.org/10.1016/j.pocean.2016.12.001.
6. Olivar, M.P.; Bernal, A.; Molí, B.; Peña, M.; Balbín, R.; Castellón, A.; Miquel, J.; Massutí, E. Vertical distribution, diversity and assemblages of mesopelagic fishes in the western Mediterranean. *Deep Sea Res. Part I Oceanogr. Res. Pap.* **2012**, *62*, 53–69. https://doi.org/10.1016/j.dsr.2011.12.014.
7. Badcock, J.; Merrett, N.R. Midwater fishes in the eastern North Atlantic—I. Vertical distribution and associated biology in 30°N, 23°W, with developmental notes on certain myctophids. *Prog. Oceanogr.* **1976**, *7*, 3–58. https://doi.org/10.1016/0079-6611(76)90003-3.
8. Battaglia, P.; Pagano, L.; Consoli, P.; Esposito, V.; Granata, A.; Guglielmo, L.; Pedá, C.; Romeo, T.; Zagami, G.; Vicchio, T.M.; et al. Consumption of mesopelagic prey in the Strait of Messina, an upwelling area of the central Mediterranean Sea: Feeding behaviour of the blue jack mackerel *Trachurus picturatus* (Bowdich, 1825). *Deep Sea Res. Part I Oceanogr. Res. Pap.* **2020**, *155*, 103158. https://doi.org/10.1016/j.dsr.2019.103158.
9. Battaglia, P.; Andaloro, F.; Esposito, V.; Granata, A.; Guglielmo, L.; Guglielmo, R.; Musolino, S.; Romeo, T.; Zagami, G. Diet and trophic ecology of the lanternfish *Electrona risso* (Cocco 1829) in the Strait of Messina (central Mediterranean Sea) and potential resource utilization from the Deep Scattering Layer (DSL). *J. Mar. Syst.* **2016**, *159*, 100–108. https://doi.org/10.1016/j.jmarsys.2016.03.011.
10. Ozawa, T.; Fujii, K.; Kawaguchi, K. Feeding chronology of the vertically migrating gonostomatid fish,*Vinciguerria nimbaria* (Jordan and Williams), off southern Japan. *J. Oceanogr.* **1977**, *33*, 320–327. https://doi.org/10.1007/BF02109577.
11. Marchal, E.; Lebourges, A. Acoustic evidence for unusual diel behaviour of a mesopelagic fish (*Vinciguerria nimbaria*) exploited by tuna. *ICES J. Mar. Sci.* **1996**, *53*, 443–447. https://doi.org/10.1006/jmsc.1996.0062.
12. Lebourges-Dhaussy, A.; Marchal, É.; MenkÈS, C.; Champalbert, G.; Biessy, B. *Vinciguerria nimbaria* (micronekton), environment and tuna: Their relationships in the Eastern Tropical Atlantic. *Oceanol. Acta* **2000**, *23*, 515–528. https://doi.org/10.1016/S0399-1784(00)00137-7.
13. Stequert, B.; Menard, F.; Marchal, E. Reproductive biology of *Vinciguerria nimbaria* in the equatorial waters of the eastern Atlantic Ocean. *J. Fish Biol.* **2003**, *62*, 1116–1136. https://doi.org/10.1046/j.1095-8649.2003.00104.x.
14. Menon, N.G.; Pillai, N.G.K.; Reghu, R.S.; Balachandran, K.K. Distribution and abundance of the genus Vinciguerria (Gonostomatidae) in the DSL of Indian EEZ with a note on the biology of *Vinciguerria nimbaria*. In Proceedings of the Second Workshop on Scientific Results of FORV Sagar Sampada, New Delhi, India, 15–17 February 1994; pp. 127–137.
15. Battaglia, P.; Ammendolia, G.; Cavallaro, M.; Consoli, P.; Esposito, V.; Malara, D.; Rao, I.; Romeo, T.; Andaloro, F. Influence of lunar phases, winds and seasonality on the stranding of mesopelagic fish in the Strait of Messina (Central Mediterranean Sea). *Mar. Ecol.* **2017**, *38*, e12459. https://doi.org/10.1111/maec.12459.
16. Ménard, F.; Marchal, E. Foraging behaviour of tuna feeding on small schooling *Vinciguerria nimbaria* in the surface layer of the equatorial Atlantic Ocean. *Aquat. Living Resour.* **2003**, *16*, 231–238. https://doi.org/10.1016/S0990-7440(03)00040-8.
17. Rosas-Luis, R.; Tafur-Jimenez, R.; Alegre-Norza, A.R.; Castillo-Valderrama, P.R.; Cornejo-Urbina, R.M.; Salinas-Zavala, C.A.; Sánchez, P. Trophic relationships between the jumbo squid (*Dosidicus gigas*) and the lightfish (*Vinciguerria lucetia*) in the Humboldt Current System off Peru. *Sci. Mar.* **2011**, *75*, 549–557. https://doi.org/10.3989/SCIMAR.2011.75N3549.
18. Battaglia, P.; Ammendolia, G.; Esposito, V.; Romeo, T.; Andaloro, F. Few but relatively large prey: Trophic ecology of *Chauliodus sloani* (pisces: Stomiidae) in deep waters of the central Mediterranean sea. *J. Ichthyol.* **2018**, *58*, 8–16. https://doi.org/10.1134/S0032945218010034.
19. Battaglia, P.; Pedà, C.; Malara, D.; Milisenda, G.; MacKenzie, B.R.; Esposito, V.; Consoli, P.; Vicchio, T.M.; Stipa, M.G.; Pagano, L.; et al. Importance of the lunar cycle on mesopelagic foraging by Atlantic bluefin tuna in the upwelling area of the Strait of Messina (Central Mediterranean Sea). *Animals* **2022**, *12*, 2261. https://doi.org/10.3390/ani12172261.
20. Battaglia, P.; Andaloro, F.; Consoli, P.; Esposito, V.; Malara, D.; Musolino, S.; Peda, C.; Romeo, T. Feeding habits of the Atlantic bluefin tuna, *Thunnus thynnus* (L. 1758), in the central Mediterranean Sea (Strait of Messina). *Helgol. Mar. Res.* **2013**, *67*, 97–107. https://doi.org/10.1007/s10152-012-0307-2.
21. Tomás, J.; Panfili, J. Otolith microstructure examination and growth patterns of *Vinciguerria nimbaria* (Photichthyidae) in the tropical Atlantic Ocean. *Fish. Res.* **2000**, *46*, 131–145. https://doi.org/10.1016/S0165-7836(00)00140-5.
22. Froese, R.; Pauly, D. FishBase. World Wide Web Electronic Publication. Version (02/2022). Available online: www.fishbase.org (accessed on 1 March 2023).

23. Sanzo, L. Sviluppo embrionale, stadi larvali, post larvali e giovanili di Sternoptychidae e Stomiatidae. Sternoptychidae. *Ichthyococcus ovatus* Cocco. *Reg. Com. Talassogr. Ital. Monogr.* **1930**, *2*, 69–119.
24. Sanzo, L. Stadi post-embrionali di *Vinciguerria attenuata* (Cocco) e *V. poweriae* (Cocco) Jordan ed Evermann. *Reg. Com. Talassogr. Ital. Mem.* **1913**, *35*, 1–8.
25. Battaglia, P.; Malara, D.; Ammendolia, G.; Romeo, T.; Andaloro, F. Relationships between otolith size and fish length in some mesopelagic teleosts (Myctophidae, Paralepididae, Phosichthyidae and Stomiidae). *J. Fish Biol.* **2015**, *87*, 774–782. https://doi.org/10.1111/jfb.12744.
26. Battaglia, P.; Malara, D.; Romeo, T.; Andaloro, F. Relationships between otolith size and fish size in some mesopelagic and bathypelagic species from the Mediterranean Sea (Strait of Messina, Italy). *Sci. Mar.* **2010**, *74*, 605–612. https://doi.org/10.3989/scimar.2010.74n3605.
27. López-Pérez, C.; Olivar, M.P.; Hulley, P.A.; Tuset, V.M. Length–weight relationships of mesopelagic fishes from the equatorial and tropical Atlantic waters: Influence of environment and body shape. *J. Fish Biol.* **2020**, *96*, 1388–1398. https://doi.org/10.1111/jfb.14307.
28. Jawad, L.A.; Sabatino, G.; Ibáñez, A.L.; Andaloro, F.; Battaglia, P. Morphology and ontogenetic changes in otoliths of the mesopelagic fishes *Ceratoscopelus maderensis* (Myctophidae), *Vinciguerria attenuata* and *V. poweriae* (Phosichthyidae) from the Strait of Messina (Mediterranean Sea). *Acta Zool.* **2018**, *99*, 126–142. https://doi.org/10.1111/azo.12197.
29. Longo, F.; Malara, D.; Stipa, M.G.; Consoli, P.; Romeo, T.; Sanfilippo, M.; Abbate, F.; Andaloro, F.; Battaglia, P. Age, growth and otolith microstructure of the spotted lanternfish *Myctophum punctatum* Rafinesque 1810. *J. Mar. Sci. Eng.* **2021**, *9*, 801. https://doi.org/10.3390/jmse9080801.
30. Le Cren, E.D. The length-weight relationship and seasonal cycle in gonad weight and condition in the perch (*Perca fluviatilis*). *J. Anim. Ecol.* **1951**, *20*, 201–219. https://doi.org/10.2307/1540.
31. Froese, R. Cube law, condition factor and weight–length relationships: History, meta-analysis and recommendations. *J. Appl. Ichthyol.* **2006**, *22*, 241–253. https://doi.org/10.1111/j.1439-0426.2006.00805.x.
32. Froese, R.; Tsikliras, A.C.; Stergiou, K.I. Editorial note on weight–length relations of fishes. *Acta Ichthyol. Piscat.* **2011**, *41*, 261–263. https://doi.org/10.3750/AIP2011.41.4.01.
33. Hebbali, A. olsrr: Tools for Building OLS Regression Models. R Package Version 0.5.3. 2020. Available online: https://CRAN.R-project.org/package=olsrr (accessed on 1 February 2023).
34. Ricker, W.E. Computation and interpretation of biological statistics of fish populations. *Bull. Fish. Res. Board Can.* **1975**, *191*, 1–382.
35. R Core Team. *R: A Language and Environment for Statistical Computing*; R Foundation for Statistical Computing: Vienna, Austria, 2022.
36. Posit Team. *RStudio: Integrated Development for R*; 2023.03.0 Posit Software; PBC: Boston, MA, USA, 2023.
37. Fox, J.; Weisberg, S. *An R Companion to Applied Regression*, 3rd ed.; SAGE Publications Inc: Thousand Oaks, CA, USA, 2019; p. 608.
38. Giragosov, V.; Ovcharov, O. Age and growth of the lantern fish *Myctophum nitidulum* (Myctophidae) from the tropical Atlantic. *J. Ichthyol.* **1992**, *32*, 34–42.
39. Bystydzieńska, Z.E.; Phillips, A.J.; Linkowski, T.B. Larval stage duration, age and growth of blue lanternfish *Tarletonbeania crenularis* (Jordan and Gilbert, 1880) derived from otolith microstructure. *Environ. Biol. Fishes* **2010**, *89*, 493–503. https://doi.org/10.1007/s10641-010-9681-2.
40. Greely, T.M.; Gartner, J.V., Jr.; Torres, J.J. Age and growth of *Electrona antarctica* (Pisces: Myctophidae), the dominant mesopelagic fish of the Southern Ocean. *Mar. Biol.* **1999**, *133*, 145–158. https://doi.org/10.1007/s002270050453.
41. Wang, Y.; Zhang, J.; Chen, Z.; Jiang, Y.; Xu, S.; Li, Z.; Wang, X.; Ying, Y.; Zhao, X.; Zhou, M. Age and growth of *Myctophum asperum* in the South China Sea based on otolith microstructure analysis. *Deep Sea Res. Part II Top. Stud. Oceanogr.* **2019**, *167*, 121–127. https://doi.org/10.1016/j.dsr2.2018.07.004.
42. Gartner, J.V. Life histories of three species of lanternfishes (Pisces: Myctophidae) from the eastern Gulf of Mexico. I. Morphological and microstructural analysis of sagittal otoliths. *Mar. Biol.* **1991**, *111*, 11–20. https://doi.org/10.1007/bf01986339.
43. Sassa, C.; Takahashi, M. Comparative larval growth and mortality of mesopelagic fishes and their predatory impact on zooplankton in the Kuroshio region. *Deep Sea Res. Part I Oceanogr. Res.* **2018**, *131*, 121–132. https://doi.org/10.1016/j.dsr.2017.11.007.
44. Katsanevakis, S.; Maravelias, C.D. Modelling fish growth: Multi-model inference as a better alternative to a priori using von Bertalanffy equation. *Fish Fish.* **2008**, *9*, 178–187. https://doi.org/10.1111/j.1467-2979.2008.00279.x.
45. Katsanevakis, S. Modelling fish growth: Model selection, multi-model inference and model selection uncertainty. *Fish. Res.* **2006**, *81*, 229–235. https://doi.org/10.1016/j.fishres.2006.07.002.
46. Gompertz, B. XXIV. On the nature of the function expressive of the law of human mortality, and on a new mode of determining the value of life contingencies. In a letter to Francis Baily, Esq. F. R. S. & c. *Philos. Trans. R. Soc. Lond.* **1825**, *115*, 513–583. https://doi.org/10.1098/rstl.1825.0026.
47. von Bertalanffy, L. A quantitative theory of organic growth (inquiries on growth laws ii). *Hum. Biol.* **1938**, *10*, 181–213. https://doi.org/10.2307/41447359.
48. Ricker, W.E. Linear Regressions in Fishery Research. *J. Fish. Res. Board Can.* **1973**, *30*, 409–434. https://doi.org/10.1139/f73-072.
49. Ogle, D.H.; Wheeler, P.; Dinno, A. *FSA: Fisheries Stock Analysis*; R Package Version 0.8.23; 2019.

50. Baty, F.; Ritz, C.; Charles, S.; Brutsche, M.; Flandrois, J.-P.; Delignette-Muller, M.-L. A Toolbox for Nonlinear Regression in R: The Package nlstools. *J. Stat. Softw.* **2015**, *66*, 1–21. https://doi.org/10.18637/jss.v066.i05.
51. Akaike, H. Information theory and an extension of the maximum likelihood principle. In Proceedings of the Second International Symposium on Information Theory, Tsahkadsor, Armenia, 2–8 September 1971; pp. 267–281.
52. Burnham, K.P.; Anderson, D.R. *Model Selection and Multimodel Inference: A Practical Information-Theoretic Approach*, 2nd ed.; Springer New York, Inc.: New York, NY, USA, 2002; Volume 67.
53. Mazerolle, M.J. AICcmodavg: Model Selection and Multimodel Inference Based on (Q)AIC(c); R Package Version 2.2.2; 2019.
54. Linkowski, T.B.; Radtke, R.L.; Lenz, P.H. Otolith microstructure, age and growth of two species of *Ceratoscopelus* (Osteichthyes: Myctophidae) from the eastern North Atlantic. *J. Exp. Mar. Biol. Ecol.* **1993**, *167*, 237–260. https://doi.org/10.1016/0022-0981(93)90033-K.
55. Linkowski, T.B. Otolith microstructure and growth patterns during the early life history of lanternfishes (family Myctophidae). *Can. J. Zool.* **1991**, *69*, 1777–1792. https://doi.org/10.1139/z91-247.
56. Suthers, I.M. Spatial variability of recent otolith growth and rna indices in pelagic juvenile *Diaphus kapalae* (Myctophidae): An effect of flow disturbance near an island? *Mar. Freshw. Res.* **1996**, *47*, 273–282. https://doi.org/10.1071/MF9960273.
57. Hosseini-Shekarabi, S.P.; Valinassab, T.; Bystydzieńska, Z.; Linkowski, T. Age and growth of *Benthosema pterotum* (Alcock, 1890) (Myctophidae) in the Oman Sea. *J. Appl. Ichthyol.* **2015**, *31*, 51–56. https://doi.org/10.1111/jai.12620.
58. Kalinina, E.; Shevchenko, N. Biology of *Vinciguerria nimbaria* (Jordan et Williams)(Gonostomidae) in the equatorial waters of the Indian Ocean. *Vopr Ikhtiologii* **1984**, *24*, 238–242.
59. Linkowski, T.B. Lunar rhythms of vertical migrations coded in otolith microstructure of North Atlantic lanternfishes, genus *Hygophum* (Myctophidae). *Mar. Biol.* **1996**, *124*, 495–508. https://doi.org/10.1007/BF00351031.
60. García-Seoane, E.; Meneses, I.; Silva, A. Microstructure of the otoliths of the glacier lanternfish, *Benthosema glaciale*. *Mar. Freshw. Res.* **2014**, *66*, 70–77. https://doi.org/10.1071/MF13211.
61. Real, E.; Bernal, A.; Morales-Nin, B.; Molí, B.; Alvarez, I.; Pilar Olivar, M. Growth patterns of the lanternfish *Ceratoscopelus maderensis* in the western Mediterranean Sea. *Sci. Mar.* **2021**, *85*, 71–80. https://doi.org/10.3989/scimar.05106.007.
62. Ricker, W.E. Growth rates and models. In *Fish Physiology, III, Bioenergetics and Growth*; Hoar, W.S., Randall, D.J., Brett, J.R., Eds.; Academic Press: New York, NY, USA, 1979; pp. 677–744.
63. Liu, K.-M.; Wu, C.-B.; Joung, S.-J.; Tsai, W.-P.; Su, K.-Y. Multi-Model Approach on growth estimation and association with life history trait for elasmobranchs. *Front. Mar. Sci.* **2021**, *8*, 591692. https://doi.org/10.3389/fmars.2021.591692.
64. Cailliet, G.; Goldman, K. Age Determination and Validation in Chondrichthyan Fishes. In *Biology of Sharks and their relatives*; Carrier J.C., Musick J.A., Heithaus M.R., Eds.; CRC Press, Boca Raton, Florida, USA, 2004; pp. 399–448. https://doi.org/10.1201/9780203491317.pt3.
65. Campana, S.E.; Thorrold, S.R. Otoliths, increments, and elements: Keys to a comprehensive understanding of fish populations? *Can. J. Fish. Aquat. Sci.* **2001**, *58*, 30–38. https://doi.org/10.1139/F00-177.
66. Nazir, A.; Khan, M.A. Stock-specific assessment of precise age and growth in the long-whiskered catfish *Sperata aor* from the Ganges River. *Mar. Freshw. Res.* **2020**, *71*, 1693–1701. https://doi.org/10.1071/MF19315.